Identifying and de-risking near-field opportunities through reliable pre-stack broadband attributes: examples from the Paleocene North Sea (UK–Norway) injectites play

NOÉMIE PERNIN*, LAURENT FEUILLEAUBOIS, TIM BIRD & CYRILLE REISER

Petroleum Geo-Services (PGS), PO Box 251 Lilleaker, 0216 Oslo, Norway

**Correspondence: noemie.pernin@pgs.com*

Abstract: Tertiary injectites, which are re-mobilized sandstones, represent commercially attractive targets for near-field, long-reach tie-backs to existing field infrastructure above and adjacent to producing reservoirs. Injectites exhibit exceptional porosity–permeability and productivity, such that discoveries can add incremental reserves and lift production decline in mature fields. Abundant injectites are visible on seismic data in the Tertiary of the Viking Graben, but, as some disappointing wells have established, not all are hydrocarbon-charged. The challenge is to reliably distinguish hydrocarbon-filled high porosity–permeability features from tight or dry reservoirs in a cost-effective way. Regional rock physics analysis of injectite reservoirs, using well data from fields in Norway and the UK, reveals that a combination of elastic attributes can effectively discriminate lithology and hydrocarbon presences in these reservoirs. After pre-stack conditioning, broadband seismic data correlate reliably with wells, giving confidence that pre-stack seismic is faithfully imaging the elastic properties of the subsurface in lower Tertiary target intervals. Informed by rock physics analysis, a combination of broadband seismic elastic attributes is used to predict sand presence and de-risk hydrocarbon presence in reservoirs v. water-wet targets. Hydrocarbon sand distribution predicted from relative acoustic impedance and V_P/V_S matches to known accumulations and identifies remaining near-field opportunities.

This paper introduces sand injectites, their petroleum potential and their characteristics in terms of rock physical properties and elastic properties that can be derived using seismic reservoir characterization. Elastic properties of representative well data from both sides of the UK–Norway border in the North Sea Viking Graben have been analysed to understand the potential to reliably differentiate injectite sand targets from surrounding shales and to de-risk the probability of hydrocarbon fill within these reservoirs. A workflow has been implemented to generate relative elastic attributes from conditioned angle stacks which were integrated with the rock physics analysis to predict injectite sand distribution and to de-risk the presence of hydrocarbons in identified injectite targets.

The commercial relevance of injectite reservoirs

The Tertiary injectites of the Viking Graben offer opportunities to add low-cost incremental production and reserves from relatively shallow targets above and adjacent to producing reservoirs and field infrastructure. The North Sea Viking Graben has been a prolific hydrocarbon province, producing principally from Jurassic, Paleocene and Eocene clastic reservoirs for more than 40 years. In this mature basin, many of the fields are in their later stages of field life and experiencing declining production, so additional near-field step-out or extended-reach targets are in demand to augment production and prolong field life.

Injected Tertiary sand bodies have been proven to hold significant amounts of hydrocarbons in the North Sea Viking Graben. Table 1 lists the volume of oil production from North Sea fields with injectite reservoirs. The injectites fields located in the Viking Graben area are highlighted in Figure 1. Wells and production data demonstrate that these injectite sands typically have exceptionally high porosity (35–40% in the Volund Field) and permeability (7 D (darcies) average permeability reported in the UK Gryphon Field in Templeton *et al.* 2006), and high net-to-gross ratios (100% in 439 m of a horizontal well in the UK Gryphon Field: Lonergan *et al.* 2007). Despite the complex nature of the reservoirs and the limited thickness of the sands, the reservoirs can be very well connected, with good aquifer support resulting in high well rates (e.g. 20 000 bbl/day in the UK Alba Field: Duranti *et al.* 2000) and high recovery factors (the Harding Field, for example, is estimated to have a recovery factor in excess

From: Patruno, S., Archer, S. G., Chiarella, D., Howell, J. A., Jackson, C. A.-L. & Kombrink, H. (eds) *Cross-Border Themes in Petroleum Geology I: The North Sea*. Geological Society, London, Special Publications, **494**, https://doi.org/10.1144/SP494-2019-11

Table 1. *Oil production from North Sea fields with injectite reservoirs*

Country	Field	Oil production* (MMbbl)
Norway†	Volund	64
Norway	Grane	750
Norway	Balder	436
Norway	Jotun	145
Norway	Sleipner East	198
UK‡	Maclure	38
UK	Gryphon	139
UK	Harding	278
UK	Leadon	18
UK	Alba	429
UK	Chestnut	22

*Oil production in millions of barrels (MMbbl) to end 2018 from government sources.
†From Norwegian Petroleum Directorate (NPD) data pages (http://factpages.npd.no/factpages/).
‡From UK Oil and Gas Authority (OGA) field data pages (https://data-ogauthority.opendata.arcgis.com/pages/production).

of 70%: Zhang *et al.* 2010). Production from the Gryphon Field was doubled late in field life by developing the thin 'wings' of the reservoir (Braccini *et al.* 2008). Field wells have demonstrated that the complex geometries of upwards-stepping sills and dykes can result in a significant column in the wings exceeding 300 m in height (Schwab *et al.* 2014). Apache announced a 362 m hydrocarbon column in their 2015 'Corona' UK discovery well 9/18a-39a,39z in injectites above the Jurassic reservoir of the Buckland Field.

Genesis and geometry of injectites

Injectites are created through post-depositional remobilization of fluidized sands injected from a 'parent' sand into surrounding stratigraphy (Huuse *et al.* 2001, 2007; Hurst & Cartwright 2007; Braccini *et al.* 2008; Hurst *et al.* 2011). Injectite sands typically exhibit complex, enigmatic geometries similar to those of igneous intrusives, with 'saucer-shaped' geometries of bedding-parallel sills and steep, subvertical dyke-like 'risers' stepping up through the stratigraphy, as illustrated in Figure 2 and imaged on seismic in Figure 3.

Seismic imaging of injectites

Such features are abundant in the Tertiary sequence of the central depocentre of the North Sea Viking Graben area. The seismic imaging challenge has been that injectites can be thin, with steep, conflicting dips, and have proved difficult to resolve and evaluate using the band-limited seismic data available in the past. This made sand injectites a challenging play to characterize, understand and exploit successfully. Before more advanced digital streamer

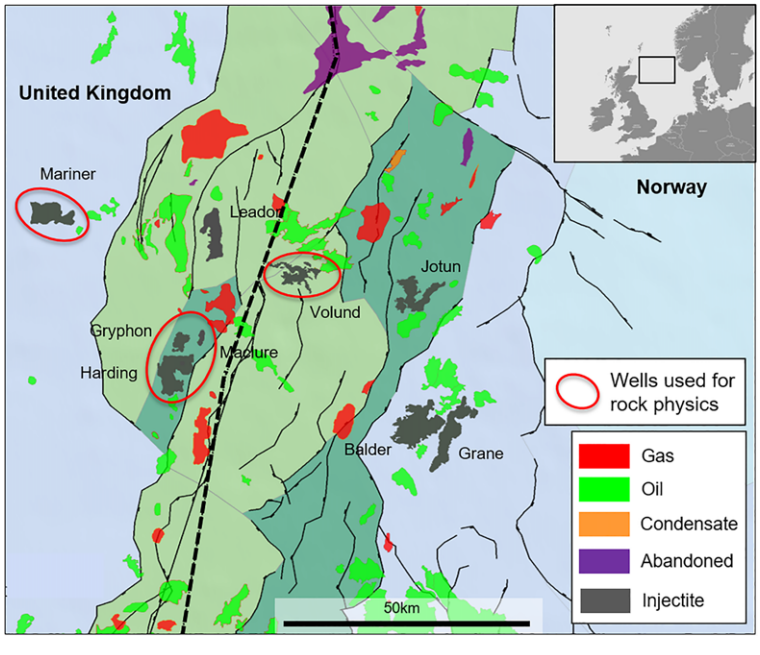

Fig. 1. Location of Tertiary injectite discoveries in North Sea Viking Graben spanning UK and Norway, and wells used in this study.

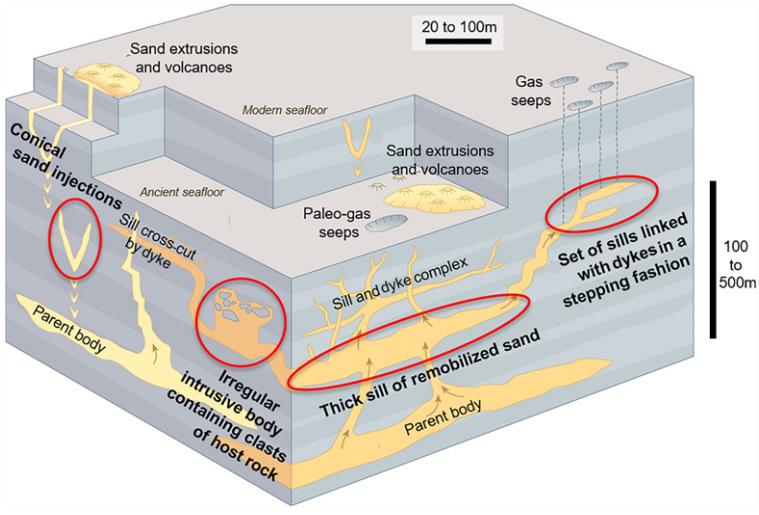

Fig. 2. Typical sand-injectite geometries and features. Red ellipses indicate common hydrocarbon trapping geometries (adapted from Hurst & Cartwright 2007).

recording and the advent of broadband seismic data acquisition in 2007, seismic data were more limited in bandwidth ('band limited'), and especially lacked the lower octaves of signal content below 6–8 Hz. Such a lack of low frequencies leads to wavelets with large side lobes that can result in false seismic horizon artefacts above and below genuine geological boundaries (ten Kroode *et al.* 2013). Predictable targeting of injectite reservoir intervals was impaired by the misleading interference of such prominent side-lobe energy as a consequence of data that was limited in bandwidth.

Broadband seismic data acquisition measures information from lower frequencies, down to 3–4 Hz, as well as additional high frequencies (the high-end frequency range varies depending on the extent of attenuation as the acoustic energy travels through the subsurface). This broader seismic bandwidth has enhanced the ability to use seismic data to de-risk lithology and hydrocarbon presence (Reiser *et al.* 2015). Improved seismic characterization and de-risking has meant that even relatively modest-sized injectite features can be commercially attractive.

The latest generation of broadband dual-sensor towed streamer seismic data (Carlson *et al.* 2007; Parkes & Hegna 2011) has enabled improved imaging and characterization of reservoirs (Reiser *et al.* 2012), and has provided pre-stack seismic data of sufficient quality (bandwidth, signal-to-noise and amplitude fidelity across all offset ranges) to enable robust seismic inversion. The resulting elastic attributes have been found to reliably identify injectite lithologies and to characterize these injectite reservoirs and fluids from seismic in order to appropriately risk potential incremental opportunities from injectite plays.

Several key aspects of broadband seismic data make this possible, including:

- Additional high and especially low frequencies (down to the 3–4 Hz range) result in wavelets with significantly less side-lobe energy, improving the interpretability of the data.
- Additional low frequencies introduce more background trend information to the seismic response allowing geological boundaries (stratigraphy and faults) to stand out more from the background.
- Additional low frequencies enable relative elastic attributes that are closer to absolute elastic properties (Reiser *et al.* 2012; Reiser & Bird 2017).

With the additional bandwidth from modern broadband seismic acquisition and advanced imaging techniques, injectite geometries can often be imaged on full-stack reflectivity images, especially where there is a strong impedance contrast. The challenge remains in differentiating which are reservoir quality sands with hydrocarbon charge, as opposed to brine-filled reservoirs.

Integrated study

This paper describes a quantitative interpretation (QI) workflow deployed to identify, characterize and de-risk injectites opportunities by integrating high-quality pre-stack broadband data with rock physics analysis from well data from fields in the UK and Norway. In this study the elastic properties of key lithologies are analysed with a particular focus on

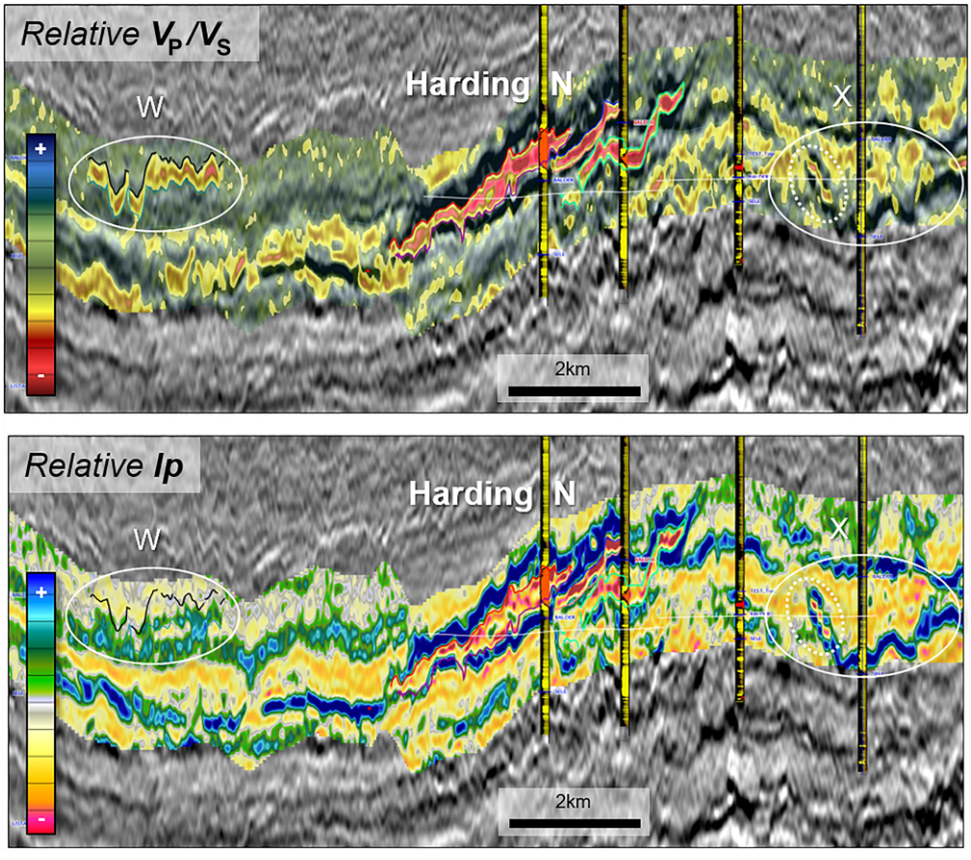

Fig. 3. Part of a regional seismic section showing full-stack seismic imaging of injectites overlain with relative acoustic impedance (Ip) and relative V_P/V_S attributes. The main field (Harding) appears as strong negative anomalies for both Ip and V_P/V_S attributes. Features highlighted in ellipses labelled X and Y denote other typical injectite geometries that can be appropriately risked for the presence of sand and hydrocarbon fill based on a combination of seismic elastic attributes. Feature X exhibits low V_P/V_S, indicative of sand, but high relative acoustic impedance suggesting brine fill; similarly for the feature marked Y, except that the upper portions of the injectite 'wing' show low impedance suggesting that the upper portions of this limb may contain hydrocarbons trapped updip.

the way these properties typically vary with depth of burial, and with different fluid content from brine to oil or gas. This understanding is then applied to diagnostic seismic elastic attributes derived from conditioned broadband angle-stack data, which are carefully tied to the available well data. The results are then mapped and integrated to define the distribution of injectite reservoir sands, and the likelihood of hydrocarbon fill within them. This workflow is represented graphically in Figure 4.

Well data used for rock physics analysis and calibration

Released well data were used in this study for calibration purposes. Well data were obtained from the Norwegian Petroleum Directorate Diskos database system (http://www.diskos.cgg.com/) and the UK Oil & Gas Authority Common Data Access (CDA) database (https://ndr.ogauthority.co.uk). The quality and quantity of well information available vary from well to well from basic log suites to detailed petrophysical and production results.

A subset of seven wells that contained usable and measured compressional and shear sonic logs, saturation, porosity, and petrophysical logs has been used in the rock physics analysis performed. Tertiary injected sandstones from wells from both the UK and Norwegian sectors in the North Sea were selected to perform a statistical depth-dependent rock physics analysis. The chosen wells contain different aged injectite reservoirs from the Mariner (Heimdal Formation sandstone), Gryphon and Volund fields (Balder

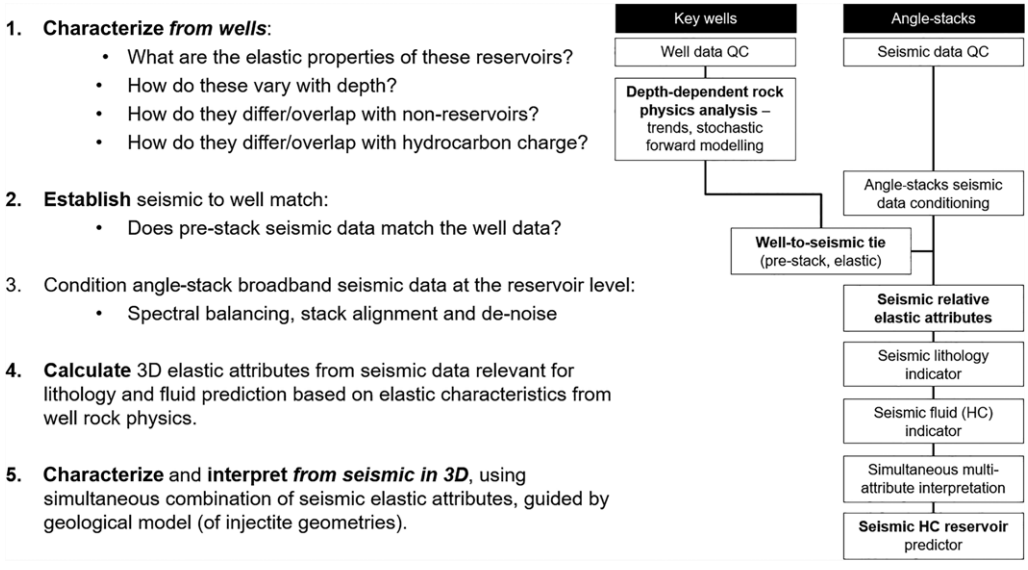

Fig. 4. Workflow to understand and appropriately risk injectites by integrating rock physics analysis of well data and pre-stack relative elastic attributes.

Formation sandstone). The fields are located 1100, 1500 and 2000 m below the seabed, respectively. The selection thus spans a depth range of approximately 1000 m, allowing a good sampling of the sandstone characteristics with depth, which is important in understanding the sensitivity of the elastic properties to burial depth. The locations of these fields from which wells were used are shown in Figure 1. Despite being buried at various depths, and being of different ages (Paleocene–Lower Eocene sands), these reservoirs exhibit consistently high porosity values of around 34%. The wells contain both hydrocarbon-filled sands and sections of brine sands. Fluid substitution using Gassmann equations (Gassmann 1951) has been used to model all sand samples back to a brine-filled state. The fluid effects on the elastic attributes have then been modelled within the reservoirs, again using Gassmann fluid substitution.

Depth-dependent rock physics analysis

At the well-log scale the rock physics analysis shows that if only acoustic impedance data are available (i.e. if no reliable velocity ratio, henceforth 'V_P/V_S', data can be obtained) it is challenging to distinguish sands from shales (Fig. 5). A cross-plot of acoustic impedance v. depth for injectite sands and surrounding shales for key wells sampling Viking Graben injectite fields in UK and Norway illustrates that there is substantial overlap between acoustic impedance values for sands and shales across a broad range of depths. If reliable V_P/V_S data can be obtained, then the right-hand cross-plot of Figure 5, showing V_P/V_S v. depth for Tertiary sands and shales with the same well data, indicates that there is a large separation between values for the two lithologies. This V_P/V_S attribute should therefore allow clear discrimination between sands and shales at all depths.

Based on the rock physics trends (mean and standard deviation/uncertainties), four lithology-fluid combinations are modelled at a range of depths with Monte-Carlo stochastic simulation (Fig. 6). This stochastic forward-modelling simulation process produces probability density functions (PDF) for any elastic properties at any depth based on the depth-dependent rock physics model. The statistical uncertainty is indicated by an uncertainty corridor of 1 SD around the mean probability distribution trend. It is at this stage that a fluid and lithology mixture can be introduced. In a cross-plot domain (most commonly using acoustic impedance (Ip) v. V_P/V_S), the PDFs are plotted as ellipses defining a standard deviation around the mean probability.

In this case, at all depths there is sufficient separation between the classes, even with an uncertainty corridor of ±1 SD. This suggests that a combination of these two attributes can discriminate with some confidence between the different lithology and fluid classes: the V_P/V_S attribute enabling separation of sand from shale; and acoustic impedance enabling discrimination of hydrocarbons from brine fill within the sand intervals. The combination of both V_P/V_S and acoustic impedance attributes is thus a

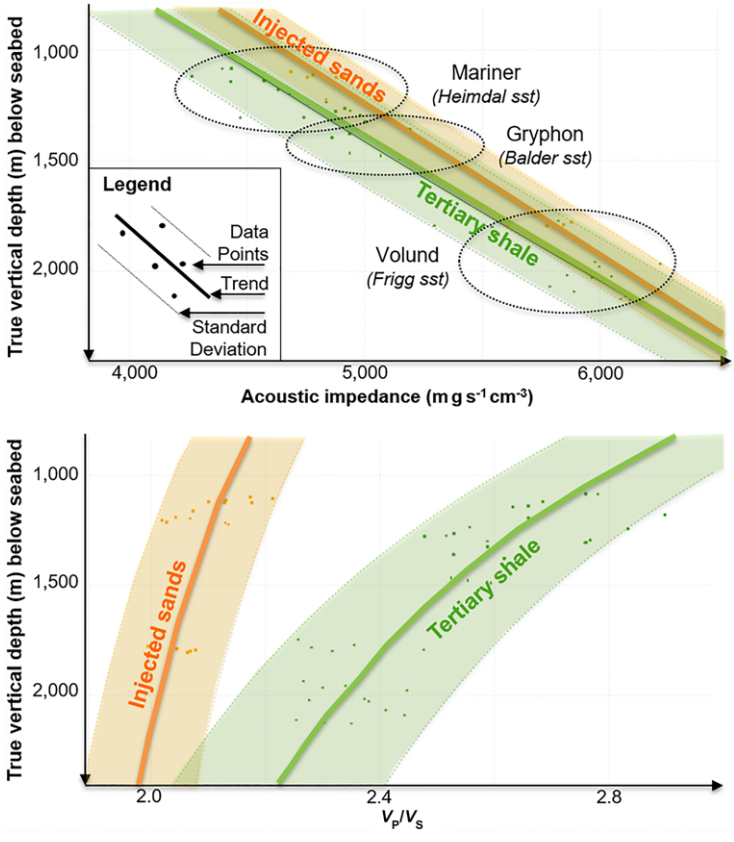

Fig. 5. Plot of acoustic impedance v. total vertical depth (metres below seabed) (left-hand graph) for injectite sands and surrounding shales for key wells sampling the Viking Graben injectite fields in the UK and Norway. With acoustic measurements only there is substantial overlap between values for sands and shales across a broad range of depths, making it challenging to discriminate sands from shales using this data type alone. The right-hand graph of V_P/V_S v. depth for the same well data indicates that this attribute allows clear discrimination between sands and shales at all depths, as there is a large separation between values for the two lithologies.

requisite to accurately identify the hydrocarbon-charged injectite sands.

Seismic inversion workflow

Seismic input

Four angle stacks (5°–15°, 15°–25°, 25°–35° and 35°–45°) from pre-stack depth-migrated seismic from large multi-client 3D surveys covering thousands of square kilometres were available as input. The data were acquired in 2013 using up to 12 dual-sensor streamers with a length of 6000 m and a shot interval of 18.75 m providing 80-fold coverage. A modern broadband pre-stack migration processing sequence was completed in 2014.

This resulted in elastic attributes with a bandwidth at the Paleocene-Eocene targets of 3–40 Hz.

Methodology

The workflow for 'sparse-spike' seismic absolute pre-stack inversion inverts simultaneously for acoustic and shear impedances using angle stacks, wavelets calculated for each angle stack and low-frequency models. The inversion uses a modern optimization engine based on developments in wavelet transform theory. A proprietary alternate-projection algorithm is used to iteratively optimize between two major constraints: the match of the synthetic model to the seismic; and the sparsity constraint. The algorithm uses Aki–Richards equations as a convolutional model and solves a constrained, non-linear optimization at every trace by matching seismic data to quantify the absolute elastic rock properties that results in the observed AVA (amplitude variation with angle) present in the input data. At the high end of the spectrum, the algorithm damps high

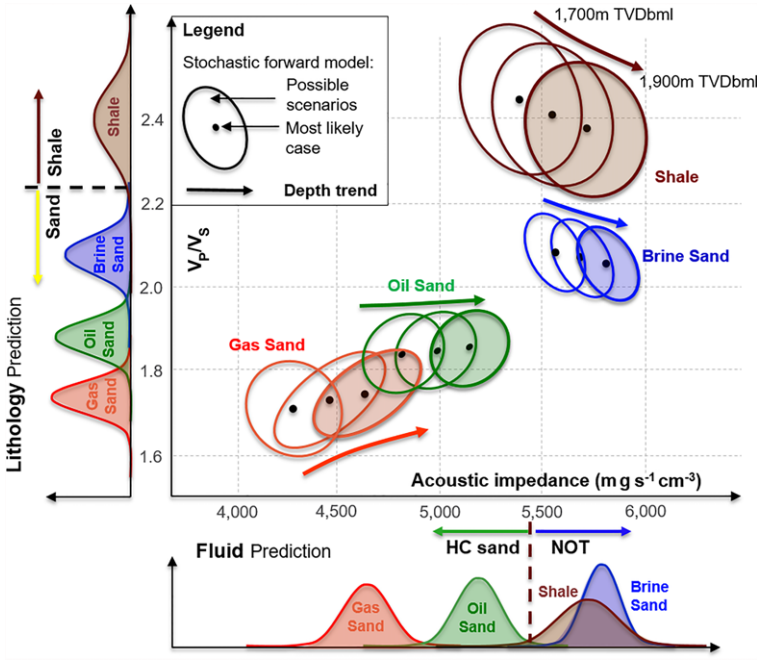

Fig. 6. Cross-plot of acoustic impedance v. V_P/V_S after Monte-Carlo simulations based on well data from the Mariner, Gryphon and Volund fields, showing the response for four distinct lithology-fluid classes, and the variation of these trends with depth. At all depths there is sufficient separation that a combination of these two attributes can discriminate with some confidence the different classes. The V_P/V_S attribute enabling separation of sand from shale. Thereafter, within the sand intervals identified from V_P/V_S, acoustic impedance enables discrimination of hydrocarbon-filled from brine-filled sands.

frequencies not constrained by the seismic while matching the low frequencies from the low-frequency models (LFMs), which cover that part of the frequency spectrum below the seismic bandwidth.

Inversion parameters and constraints

Wavelets were calculated around the target interval for each angle stack, using a statistical method that is based on seismic data only. This approach assumes zero-phase data. Long wavelets of at least 300 ms are required to capture the low-frequency–long-wavelength component of the broadband seismic data.

These LFMs are required for the inversion in order to correctly scale acoustic impedance (Ip) v. shear impedance (Is). The LFMs (Ip and Is) were based on seismic processing velocities, with a constant average density and V_P v. V_S relationship for shale estimated from well logs and validated by Greenberg–Castagna's equation (Castagna *et al.* 1985; Greenberg & Castagna 1992). An additional geophysical constraint was added to only include inversion results where Ip and V_P/V_S are between physically reasonable values of $4000 < \text{Ip} < 10\ 000$ m g s^{-1} cm^{-3} and $1.4 < V_P/V_S < 3.5$.

Once the background trends are understood and the elastic attributes scaled, relative products are generated. This is done in order to remove the uncertainties linked to the simple assumptions of the LFMs which impact the absolute values of the resultant absolute elastic attributes produced.

Limitations and pitfalls of the method

- While some care has been taken to optimize the seismic data and in testing parameters to achieve an acceptable result, this inversion workflow is applied to a large multi-client 3D dataset covering thousands of square kilometres, over which there will be significant lateral and vertical variation. The inversion parameters tested cannot be expected to be optimal over such a large and variable region. Although generally robust, seismic elastic attributes are fit-for-purpose for reconnaissance screening and high grading of opportunities, but would require further refinement over a smaller prospect area to optimize for the next

stage of deeper analysis focused on a specific local target.

- A limitation of the method used here lies in the relative nature of the inversion products. Relative inversion products represent the vertical relative changes of rock properties, and therefore interfaces, without a long-wavelength background trend of (generally) increasing values with depth.
- Rock physics analysis is constrained by limited publicly available well data, and wells with reliable dipole shear sonic measurements over significant depth intervals outside the reservoir are rare. Additional wells, especially those with shear sonic information, would be desirable.
- Wavelet estimation with broadband seismic data requires long wavelet length. This in turn necessitates long intervals of measurement in well logs for Bayesian wavelet extraction. This technique allows a phase estimation, calibrated from the well data. Unfortunately, the limited length and amount of shear sonic logs renders this approach unworkable in this case.
- A very simple rock physics model is presented here, distinguishing between only two lithologies (sand or shale) and three fluids (oil, gas or brine). The interpretation of the attributes is made here assuming that limited combinations of lithologies with fluids are possible.
- More extended rock physics analysis including more lithologies could be considered for more detailed interpretation at a smaller scale. Specifically, cemented sands should be considered separately, and the ages and compositions of sands could be further examined.
- More refined analysis may distinguish more than one shale trend from shales with different properties and ages.
- Fluid information is limited, and the sensitivity to this could be further explored. Particularly the sensitivity to oil gravity and gas–oil ratio (GOR).
- Isolated sand bodies can become overpressured with deeper burial. The effects of pressure on the elastic attributes have not been modelled.

Uncertainties

Relative seismic-based-only inversion relies on the scaling of shear and acoustic reflectivities to derive the V_P/V_S attribute. The availability of shear information from well data is key to this. If enough knowledge can be obtained from nearby well data, a location-specific V_P/V_S relation can be derived which will be more appropriate to the area of interest than the use of generic trends from Greenberg–Castagna equations. Even the trends derived from local well-data calibration points carry a degree of geostatistical uncertainty associated with the uneven spread of well control, biased to highs or 'sweet spots' adding more uncertainties to the scaling of V_P/V_S.

Furthermore, elastic properties like the relationship between V_P and V_S vary both laterally and vertically with depth, so that ideally a spatially variant scaling volume would be used rather than applying a single linear scaling relationship to the entire shear impedance volume.

Downton *et al.* (2000) provides a useful review of pitfalls of AVO (amplitude v. offset) interpretation.

Lithology and fluid prediction using seismic attributes

The rock physics analysis indicated that lithology and fluids can be discriminated from the elastic attributes: acoustic impedance and V_P/V_S. These elastic attributes can be independently computed from the seismic data alone, with well data used only to validate seismic inversion results at the well locations. A good match at many different well-calibration points gives confidence in the quality of the elastic attributes away from well control. The low frequencies present in the broadband seismic data are valuable for seismic-based inversion as they allow an increase in the frequency bandwidth that can be inverted from seismic data and therefore bring more measured information into the elastic attributes. Reliable volumes of acoustic impedance and V_P/V_S using broadband seismic inversion enable the possibility of 3D lithology and fluid prediction.

A number of reference publications by Reiser *et al.* (2012, 2015; Reiser & Bird 2017) describe the benefits to seismic inversion of the additional low frequencies from broadband seismic data, and its successful application in a range of geological settings and exploration challenges.

The methodology for integration of well rock physics data and seismic inversion data is well established, and summarized in compendia such as Avseth *et al.* (2005) and Simm & Bacon (2014). The stochastic prediction of reservoir elastic properties is discussed in more detail in a number of publications by Buland & Omre (2003*a*, *b*, *c*), Buland *et al.* (2008), Ulvmoen & Omre (2010) and Hammer *et al.* (2012).

Well to seismic integration

The availability of low-frequency information delivered by broadband seismic data enables the derivation of seismic-driven pre-stack relative inversions without the use of any well input (Reiser *et al.* 2015). Elastic properties can be estimated more reliably through a quantitative interpretation workflow (Özdemir 2009; Farouki *et al.* 2010; Reiser & Bird 2017).

The validity of the inversion results is confirmed with excellent well ties to the pre-stack broadband seismic elastic attributes, even though the well data have not been used in generating the seismic inversion attributes (Fig. 7). Figure 8 emphasizes the good tie between relative acoustic impedance from the wells and from the seismic data (left part), and the quality of the seismic-derived V_P/V_S attribute for lithology prediction (match between low V_P/V_S red values with gamma-ray (GR) and resistivity values for sands) at the injectites level.

The strong correlation of well elastic attributes to elastic attributes from pre-stack inversion of the broadband seismic data suggests that with such high-quality, conditioned dual-sensor pre-stack data, elastic attributes should be capable of discriminating both lithology and fluids in many cases.

This workflow is illustrated for two field and prospect examples:

Example 1: Volund Field, Norway

A case example across the Volund Field in Norway shows that complex geometries of hydrocarbon-filled injectite reservoirs are well imaged by the combination of elastic attributes (Figs 9 & 10). The injectite complex was identified on seismic, and seismic data have been used to successfully locate horizontal production wells (Schwab *et al.* 2014).

For this dataset, several broadband datasets covering the Viking Graben have been unified and processed together using advanced depth-imaging workflows consisting of anisotropic velocity model building and Kirchhoff depth migration including compensation for Earth absorption. The PGS complete wavefield imaging (CWI) processing workflow was implemented (Rønholt *et al.* 2015), including full waveform inversion (FWI) and separated wavefield imaging (SWIM) in order to address the imaging challenges related to lateral variation in shallow geology, such as shallow channels, with strong lithology contrasts (Ciotoli *et al.* 2016 describes this processing workflow applied to this dataset). The detailed geometries of Late Eocene V-shaped injected sands were characterized and manually inserted as geobodies into the velocity model. This corrects for local velocity anomalies associated with these shallow channels, which can otherwise distort the imaging of deeper targets. The more detailed shallow velocity model contributed to a superior final image of underlying features such as the targeted Paleocene injectites. In addition to this, detailed quality-controlled AVO analysis was performed throughout the processing, along with reservoir-orientated processing

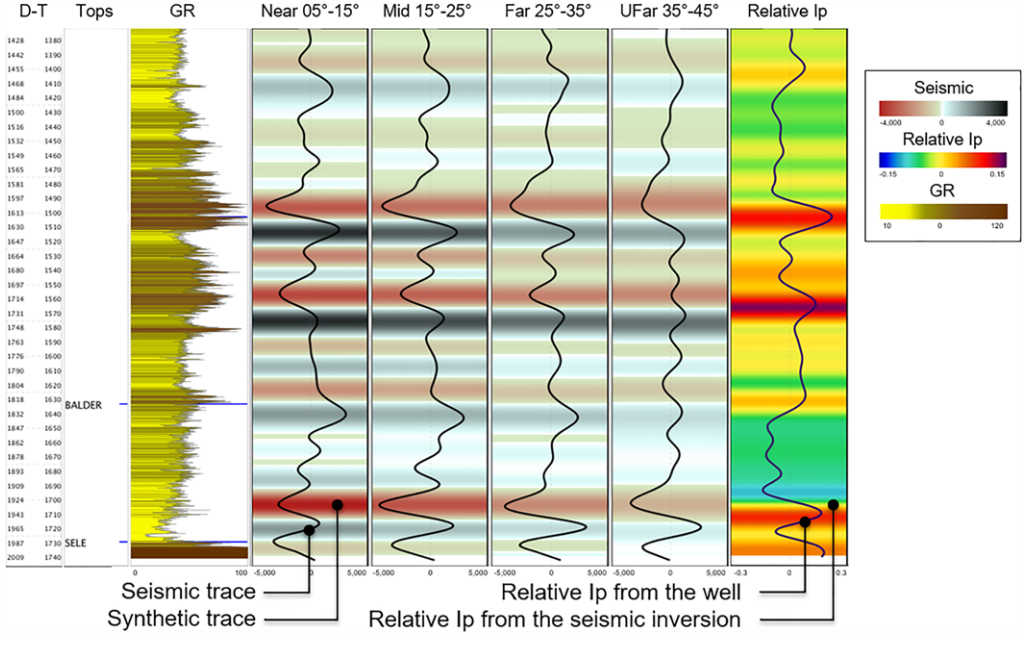

Fig. 7. Example 1 is of a pre-stack well-to-seismic tie showing a good match between the seismic angle stacks and the synthetic traces at the well location. The right-hand track shows one of the elastic attributes computed from the well logs (band-limited to match the seismic bandwidth) overlain with the same attribute from the seismic inversion (relative Ip is displayed in this example). A good match between well and seismic elastic attributes validates the robustness of the seismic inversion results.

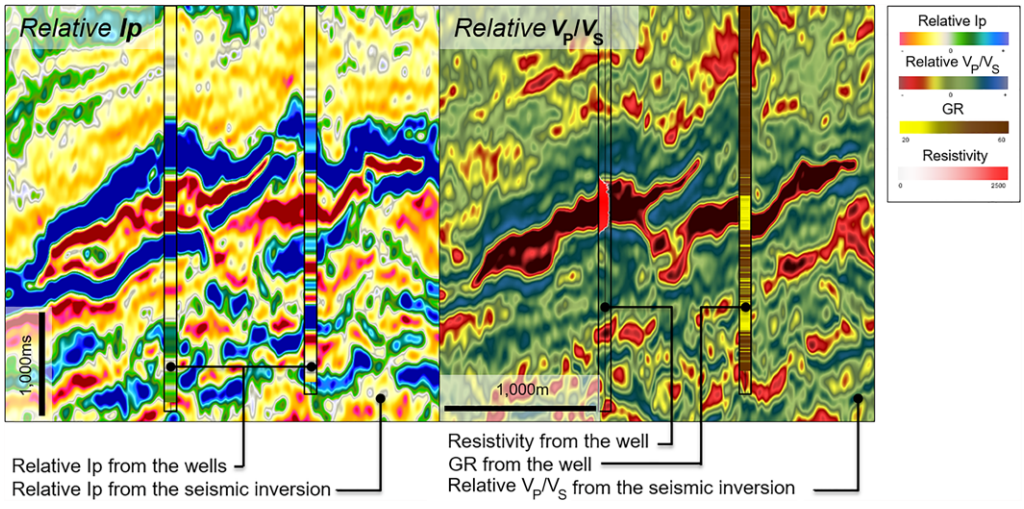

Fig. 8. Example 2 is of a pre-stack well-to-seismic tie showing a good match between the seismic inversion results and the well data with focus on one injectite. The left-hand display shows relative acoustic impedance computed from the well logs (band-limited to match the seismic bandwidth) overlain with the same attribute from the seismic inversion. The right-hand display shows low relative V_P/V_S matching with the gamma-ray (GR) and resistivity curves of the injected sands.

(additional post-migration seismic conditioning specific to the reservoir target), Angle-stack conditioning comprised spectral balancing, stack alignment and de-noising. This aims to optimize AVO-compliant angle-stack volumes for quantitative interpretation and inversion.

The rock physics analysis indicates that low V_P/V_S values can be isolated as likely sand lithology (Fig. 9). Therefore, a low V_P/V_S interval has been interpreted (red values), and top and base horizons picked to define the envelope of injectite sand. This interpretation is confirmed by the blind well ties in this section. This sand interval is then overlain on the relative impedance section illustrated in Figure 10. Low acoustic impedance (orange-red) within the sand interval defined from low V_P/V_S (black outlined bodies) is predicted to indicate hydrocarbon sands. This elastic response is confirmed to correspond to the oil-bearing injectite sand interval in the wells, with a switch to higher impedance (green-blue) below the oil–water contact (OWC) in the right-hand feature penetrated by the wells.

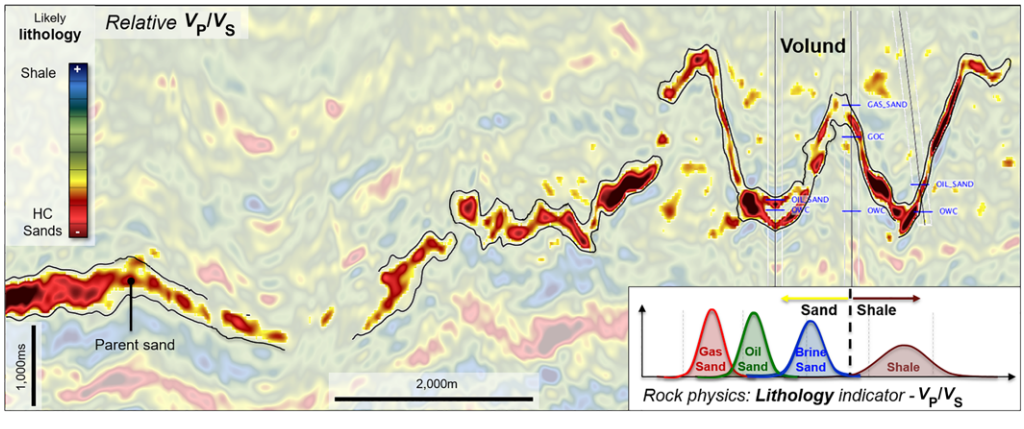

Fig. 9. Relative V_P/V_S seismic section through the Volund Field – low V_P/V_S corresponds to injectite sand interval in wells. As indicated by the rock physics analysis, low V_P/V_S values can be isolated as likely sand lithology.

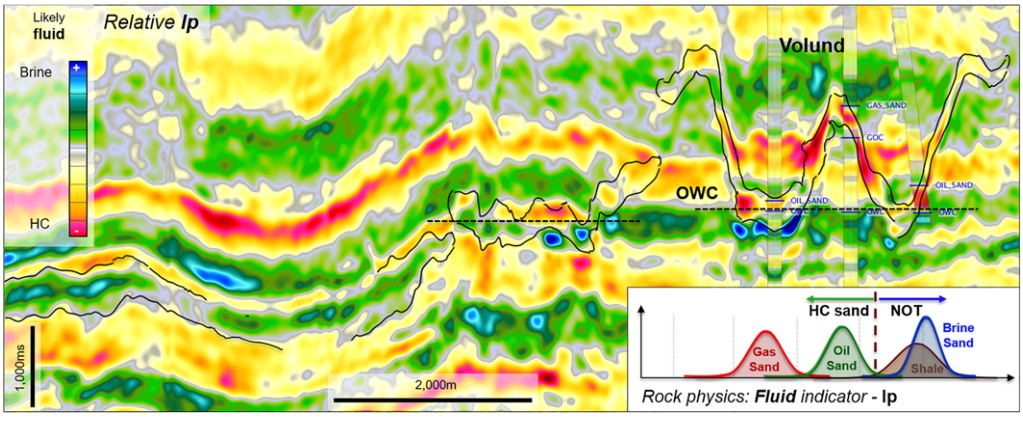

Fig. 10. Relative acoustic impedance seismic section through the Volund Field – low acoustic impedance (orange-red) within the sand interval defined from low V_P/V_S (black outlined bodies) corresponds to hydrocarbon-bearing injectite sand interval in wells, with a switch to higher impedance (green-blue) occurring below the OWC. This is confirmed by the well tied to the attributes showing a good match with the OWC position at the well location as indicated on resistivity logs.

Example 2: De-risking injectite anomalies in the Maclure area, UK

The same approach has been applied to potential near-field exploration opportunities east of the Maclure Field. These seismic data were acquired in 2013 using a multi-sensor towed streamer acquisition system, with an advanced processing flow including wavefield separation and Kirchhoff pre-stack migration. Post-migration, angle-stack conditioning comprised spectral balancing, stack alignment and de-noising.

Here a number of injectite features were identified (injectite clusters A, B and C in Figs 11 & 12). The assessment suggested that one prospect exhibited the expected combination of elastic attributes (acoustic impedance and V_P/V_S) to suggest an oil-filled reservoir (low V_P/V_S and low Ip), while the adjoining features, also diagnosed as injectite sands, were judged to be higher risk as they showed the elastic characteristics of water-wet sands (low V_P/V_S but high Ip). Reliable broadband entirely seismic-driven inversion combined with rock physics analysis have been used to de-risk the opportunities.

Figure 11 shows a relative V_P/V_S section in depth across three groups of injectite features: A, B and C. Based on the rock physics analysis (see the inset

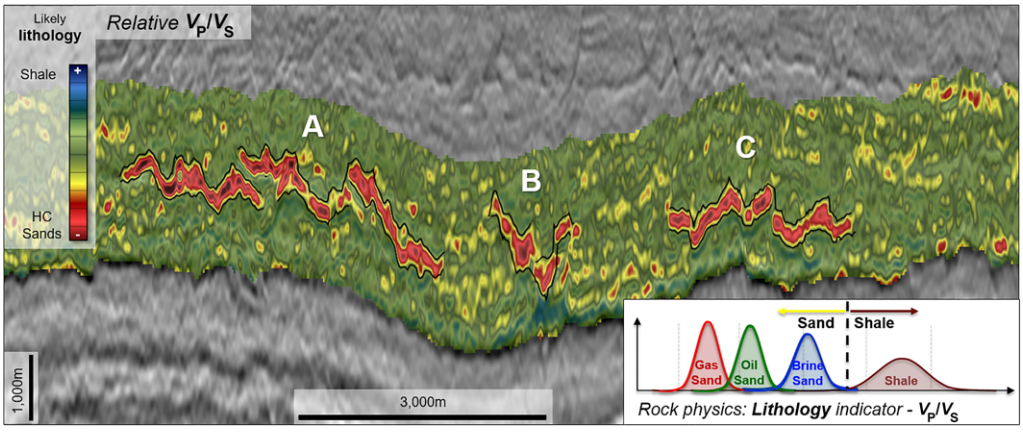

Fig. 11. Relative V_P/V_S depth section across three groups of injectite features: A, B and C. Based on the rock physics analysis (see the inset cross-plot) the lowest V_P/V_S values can be confidently characterized as sand lithology, and top and base picked.

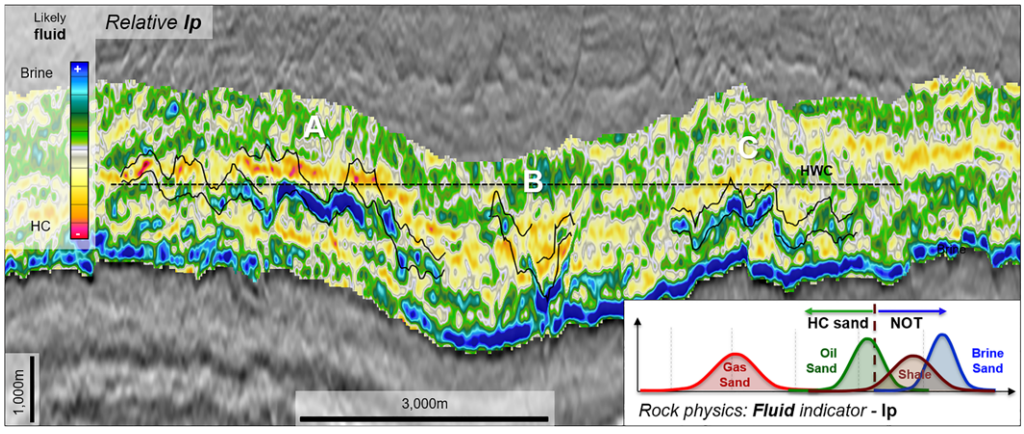

Fig. 12. Relative acoustic impedance of the same depth section across the three groups of injectite features, with the top and base of the sand interval picked (black outlines) based on V_P/V_S values (see Fig. 11). Within this sand interval in the upper portion of the left-hand injectite group A, there is a band of low impedance values suggestive of hydrocarbon fill, based on the rock physics analysis (see the inset cross-plot). There is transition below an approximately flat boundary to higher impedance values likely to indicate brine fill. These features appear to offer low-risk near-field potential for hydrocarbon-filled sands. By contrast, the other two features, B and C, show an ambiguous or high impedance response suggesting that they are water-wet sands and therefore high-risk exploration targets.

cross-plot), the lowest V_P/V_S values can be confidently characterized as sand lithology, and top and base picked.

Figure 12 shows the equivalent relative acoustic impedance across the three groups of injectite features, with the top and base of the sand interval picked (black outlines) based on V_P/V_S. Within this sand interval in the upper portion of the left-hand injectite cluster A, there is a band of low-impedance values suggestive of hydrocarbon fill, based on the rock physics analysis. There is a transition below an approximately flat boundary to higher impedance values likely to indicate brine fill. This feature appears to offer a low-risk near-field potential for hydrocarbon-filled sands; by contrast the other two features, B and C, show an ambiguous or high-impedance response suggesting that they are water-wet sands and therefore high-risk exploration targets.

Although not used in the rock physics analysis or to generate the seismic elastic attribute volumes, a well on the right-hand flank of the A feature penetrated a 55 m interval of sand with porosities ranging from 24 to 34% that tested oil and which indicated an OWC contact.

The predicted reservoir and hydrocarbon distribution of these injectite features can be reliably mapped in 3D, as illustrated in Figure 13. This 3D map shows values of acoustic impedance, diagnostic of hydrocarbon sands, occurring within geobodies defined where low V_P/V_S indicates probable sands. The Maclure Field, the 2015 Corona discovery and a 1976 discovery on the flanks of feature A all show low-impedance values indicative of hydrocarbon fill. Other similar features could be de-risked in the same way.

Figure 14 shows the improvement in this analysis which results from using broadband data. A comparison is shown of a V_P/V_S attribute extraction around the Balder injectite interval based on acquired broadband data (on the right-hand side), and the same data band limited on the low side to typical 'band-limited' lower-frequency limits (the image on the left). With the broadband data, the injectite geometries can be identified, mapped and appropriately risked. The 2015 Corona discovery defined on this dataset is clearly visible, as is the prominent feature in the foreground, which was clipped by an early well that encountered 55 m of oil-bearing sands; by contrast, for the case where the data have a 10 Hz low-cut filter applied on the low side, most of the key features are obscure and, on the basis of such data, would be considered high risk.

Conclusions

Acquired multi-sensor broadband seismic pre-stack migrated data significantly improve the imaging of the Tertiary injectite reservoirs of the North Sea. The geological understanding of injectites has improved alongside awareness of their commercial potential, especially as shallow, near-field, step-out targets have been revealed. The robust pre-stack elastic attributes derived for the Tertiary injectites studied

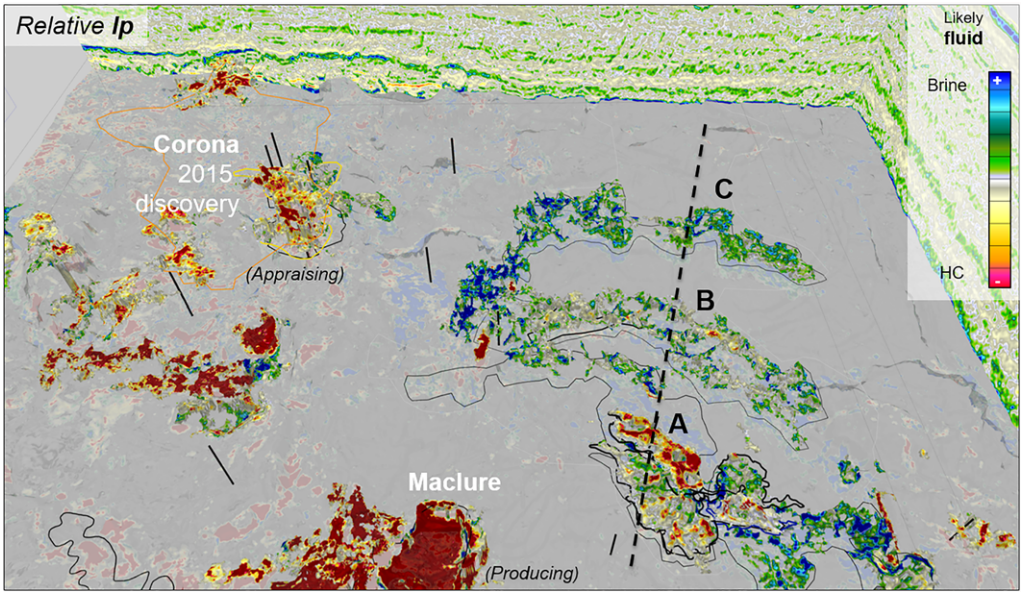

Fig. 13. 3D map view of area illustrated in Figures 11 and 12 showing values of acoustic impedance within geobodies defined where low V_P/V_S values indicate sands (the line of section for Figs 11 & 12 is shown as a dotted line). Maclure Field, 2015 Corona discovery and 1976 discovery on flanks of feature A all show low impedance values indicative of hydrocarbon fill. Other similar features could be de-risked in the same way.

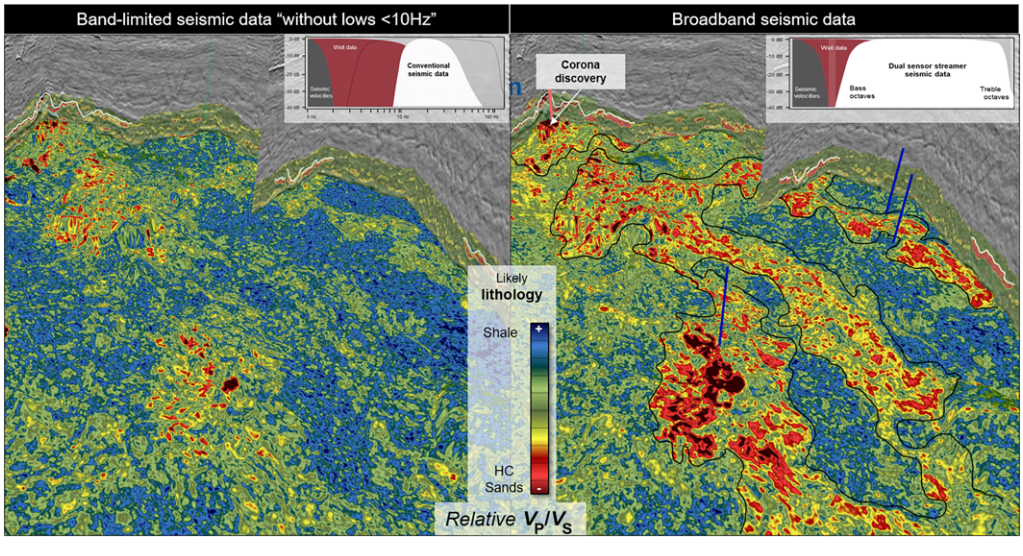

Fig. 14. Comparison of a V_P/V_S attribute extraction around the Balder Formation injectite interval based on acquired broadband data on the right-hand side, where the injectite geometries can be identified, mapped and appropriately risked. The 2015 Corona discovery defined on this dataset is clearly visible, as is the prominent feature in the foreground, which was clipped by an early well that encountered 55 m of oil-bearing sands; the image on the left is the same data band limited on the low-frequency side. Most of the key features are obscure and/or high risk based on this equivalent of conventional data.

in the UK–Norway Viking Graben have enabled reliable characterization of reservoir lithologies and the de-risking of fluid type, based on understanding of their elastic properties from a rock physics analysis of wells penetrating injectite fields. The seismic elastic attributes from pre-stack inversion show good correlation with well data, and allow effective screening of injectite opportunities. More detailed analysis would be required based on localized optimization of inversion parameters and additional well input into the rock physics model to refine the assessment of any high-graded opportunities.

Rock physics analysis using appropriate key wells from the UK and Norwegian Viking Graben indicates that good lithology and fluid discriminations can be expected using elastic attributes, supporting the predictive potential of reliable broadband seismic elastic inversion.

The remobilized injected sandstones in the Tertiary of the Viking Graben exhibit high porosity and permeability. Even modest-sized injectite features can represent attractive, relatively shallow, near-field objectives due to their known high producing rates and proximity to existing infrastructure. The new broadband data highlight many remaining untested injectite features that can be confidently characterized and de-risked using relative pre-stack attributes.

Acknowledgements The authors would like to thank PGS for permission to publish this work.

Funding This research received no specific grant from any funding agency in the public, commercial, or not-for-profit sectors.

Author contributions NP: Formal Analysis (Equal), Writing – Original Draft (Equal); LF: Formal Analysis (Equal); TB: Formal Analysis (Equal), Writing – Original Draft (Equal); CR: Formal Analysis (Lead), Supervision (Lead), Writing – Review & Editing (Lead).

References

Avseth, P., Mukerji, T. & Mavko, G. 2005. *Quantitative Seismic Interpretation – Applying Rock Physics Tools to Reduce Interpretation Risk*. Cambridge University Press, Cambridge.

Braccini, E., De Boer, W., Hurst, A., Huuse, M., Vigorito, M. & Templeton, G. 2008. Sand injectites. *Oilfield Review*, **20**, 34–49.

Buland, A. & Omre, H. 2003*a*. Bayesian linearized AVO inversion. *Geophysics*, **68**, 185–198, https://doi.org/10.1190/1.1543206

Buland, A. & Omre, H. 2003*b*. Bayesian wavelet estimation from seismic and well data. *Geophysics*, **68**, 2000–2009, https://doi.org/10.1190/1.1635053

Buland, A. & Omre, H. 2003*c*. Joint AVO inversion, wavelet estimation and noise-level estimation using a spatially coupled hierarchical Bayesian model. *Geophysical Prospecting*, **51**, 531–550, https://doi.org/10.1046/j.1365-2478.2003.00390.x

Buland, A., Kolbjørnsen, O., Hauge, R., Skjaeveland, Ø. & Duffaut, K. 2008. Bayesian lithology and fluid prediction from seismic prestack data. *Geophysics*, **73**, C13–C21, https://doi.org/10.1190/1.2842150

Carlson, D., Long, A., Söllner, W., Tabti, H., Tenghamn, R. & Lunde, N. 2007. Increased resolution and penetration from a towed dual-sensor streamer. *First Break*, **26**, 71–77.

Castagna, J.P., Batzle, M. & Eastwood, R.L. 1985. Relationships between compressional-wave and shear-wave velocities in clastic silicate rocks. *Geophysics*, **50**, 571–581, https://doi.org/10.1190/1.1441933

Ciotoli, M., Beaumont, S., Oukili, J., Korsmo, Ø., O'Dowd, N., Rønholt, G. & Dirks, V. 2016. Dual-sensor data and enhanced depth imaging sheds new light onto the mature Viking Graben area. *First Break*, **34**, 73–79.

Downton, J., Russell, B. & Lines, L. 2000. *AVO for Managers: Pitfalls and Solutions*. CREWES Research Report 12.

Duranti, D., Hurst, A., Hanson, R., Bell, C. & MacLeod, M. 2000. Reservoir characterisation of a remobilised sand-rich turbidite reservoir: the Alba Field. Paper X-05 presented at the 62nd EAGE Conference & Technical Exhibition, 29 May–2 June 2000, Glasgow, UK.

Farouki, M., Long, A. & Tenghamn, R. 2010. Enhanced resolution, imaging and interpretability: dual-sensor towed streamer data examples from around the World. *Geohorizons*, **15**, 19–23.

Gassmann, F. 1951. Elastic waves through a packing of spheres. *Geophysics*, **16**, 673–685, https://doi.org/10.1190/1.1437718

Greenberg, M.L. & Castagna, J.P. 1992. Shear-wave velocity estimation in porous rocks: theoretical formulation, preliminary verification and applications. *Geophysical Prospecting*, **40**, 195–209, https://doi.org/10.1111/j.1365-2478.1992.tb00371.x

Hammer, H., Kolbjørnsen, O., Tjelmeland, H. & Buland, A. 2012. Lithology and fluid prediction from prestack seismic data using a Bayesian model with Markov process prior. *Geophysical Prospecting*, **60**, 500–515, https://doi.org/10.1111/j.1365-2478.2011.01012.x

Hurst, A. & Cartwright, J. (eds) 2007. *Sand Injectites: Implications for Hydrocarbon Exploration and Production*. AAPG Memoirs, **87**.

Hurst, A., Scott, A. & Vigorito, M. 2011. Physical characteristics of sand injectites *Earth-Science Reviews*, **106**, 215–246, https://doi.org/10.1016/j.earscirev.2011.02.004

Huuse, M., Duranti, D., Cartwright, J., Hurst, A. & Cronin, B. 2001. Seismic expression of large-scale sand remobilisation and injection in Paleogene reservoirs of the North Sea Basin and beyond. Paper presented at the 63rd EAGE Conference & Exhibition, 11 June 2001.

Huuse, M., Cartwright, J.A., Duranti, D., Hurst, A. & Steinsland, N. 2007. Seismic characterization of large-scale sandstone intrusions. *In*: Hurst, A. & Cartwright, J. (eds) *Sand Injectites: Implications For*

Hydrocarbon Exploration and Production. AAPG Memoirs, **87**, 21–35, https://doi.org/10.1306/1209847M873253

Lonergan, L., Borlandelli, C., Taylor, A., Quine, M. & Flanagan, K. 2007. The three-dimensional geometry of sandstone injection complexes in the Gryphon Field, United Kingdom North Sea. *In*: Hurst, A. & Cartwright, J. (eds) *Sand Injectites: Implications for Hydrocarbon Exploration and Production*. AAPG Memoirs, **87**, 103–112, https://doi.org/10.1306/1209854M873260

Özdemir, H. 2009. Unbiased deterministic seismic inversion: more seismic, less model. *First Break*, **27**, 43–50.

Parkes, G. & Hegna, S. 2011. An acquisition system that extracts the earth response from seismic data. *First Break*, **29**, 81–87.

Reiser, C. & Bird, T. 2017. Broadband seismic – what are the benefits and pitfalls for E&P geoscience workflows. Presented at the AAPG International Conference & Exhibition, 15–18 October 2017, London, UK.

Reiser, C., Bird, T., Engelmark, F., Anderson, E. & Balabekov, Y. 2012. Value of broadband seismic for interpretation, reservoir characterization and quantitative interpretation workflows. *First Break*, **30**, 67–75.

Reiser, C., Bird, T. & Whaley, M. 2015. Reservoir property estimation using only dual-sensor seismic data – a case study from the West of Shetlands, UKCS. *First Break*, **33**, 93–101.

Rønholt, G., Korsmo, Ø., Naumann, S., Marinets, S., Brenne, E. & Faheem, M. 2015. Complete wavefield imaging for lithology and fluid prediction in the Barents Sea. *In*: *SEG Technical Program Expanded Abstracts 2015*. Society of Exploration Geophysicists (SEG), Tulsa, OK, 4070–4074.

Schwab, A., Jameson, E. & Townsley, A. 2014. Volund Field: development of an Eocene sandstone injection complex, offshore Norway. *In*: McKie, T., Rose, P.T.S., Hartley, A.J., Jones, D.W. & Armstrong, T.L. (eds) *Tertiary Deep-Marine Reservoirs of the North Sea Region*. Geological Society, London, Special Publications, **403**, 247–260, https://doi.org/10.1144/SP403.4

Simm, R. & Bacon, M. 2014. *Seismic amplitude – An interpreter's handbook*. Cambridge University Press, Cambridge.

Templeton, G., McInally, A., Melvin, A. & Batchelor, T. 2006. Comparison of Leadon and Gryphon fields sand injectites: Occurrence and performance. Paper presented at the 68th EAGE Conference and Exhibition incorporating SPE EUROPEC 2006, 12–15 June 2006, Vienna, Austria.

ten Kroode, F., Bergler, S., Corsten, C., de Maag, J.W., Strijbos, F. & Tijhof, H. 2013. Broadband seismic data – The importance of the low frequencies. *Geophysics*, **78**, WA3–WA14, https://doi.org/10.1190/geo2012-0294.1

Ulvmoen, M. & Omre, H. 2010. Improved resolution in Bayesian lithology/fluid inversion from prestack seismic data and well observations: part 1 – methodology. *Geophysics*, **75**, R21–R35, https://doi.org/10.1190/1.3294570

Zhang, P., Green, S. & Sharpe, A. 2010. Harding field: life extension of oil production in a low gas price world. Paper presented at the DEVEX Conference, 12–13 May 2010, Aberdeen, UK.